JOURNAL OF MATERIALS SCIENCE 30 (1995) 151–161

Surface fatigue in ceria-stabilized polycrystalline tetragonal zirconia between room temperature and 1073 K

M.-O. GUILLOU, J. L. HENSHALL, R. M. HOOPER
School of Engineering, University of Exeter, Exeter, Devon, EX4 4QF, UK

An investigation has been conducted to study the fatigue deformation and fracture induced by pressing 120° hardened silver steel conical tips against a flat, polished CeTZP counterface between 293 and 1073 K with cyclic loads of 19.6 ± 9.8 N, for up to 475 000 cycles. The ground tips of the cones plastically deformed during the initial loading cycle to produce a flattened end which conformed with the substrate. This test format has been devised to be comparable to the service conditions that these types of ceramics are likely to experience. At temperatures up to, and including, 673 K, the sequence of events is that a tetragonal to monoclinic transformed zone is formed around the contact zone. This expands as the number of cycles is increased. Much later in the fatigue process, grain lifting occurs at the periphery of the contact zone. This subsequently causes intergranular pitting to progress around the edge of the contact zone followed by extension both away from and into the contact region. At 673 K and above, a small number (3–5) of radial intergranular cracks are formed after a few cycles ($\leqslant 10$) which propagate a substantial distance away from the contact zone.

1. Introduction

Many of the engineering ceramic materials considered for use as structural components, e.g. bearings, will be required to sustain the application of compressive forces of varying magnitudes for many cycles at both ambient and elevated temperatures. Ceria-stabilized polycrystalline tetragonal zirconia, CeTZP, exhibits the highest room-temperature toughness obtainable in a monolithic ceramic [1], and does not suffer the environmental degradation problems in steam at 400–500 K reported for other toughened zirconia ceramics. The development phase of these ceramics has concentrated on producing materials with maximum toughness and strength. However, the importance of mechanical fatigue in many operational situations is now recognized, and several recent studies have demonstrated the existence of fatigue, and fatigue crack growth, in zirconia ceramics at room temperature, when subjected to tensile loading [2–8].

Many applications of ceramics involve subjecting the components to primarily compressive loading. Previous work in this respect has invoked the use of reciprocating sliding fatigue [9, 10], or repeated indentation using Vickers diamond indentors [11, 12]. In this latter case, the extremely high localized plastic strains are not representative of typical applications, and in the former case the behaviour may be dominated by adhesion between the surfaces [9]. Therefore, a novel test procedure has been developed [13] to assess the fatigue behaviour of ceramics, initially MgO but in this case CeTZP, when repeatedly elastically loaded in compression by a softer (metallic) counterface, at temperatures up to 1073 K.

In this study, 120° apical angle ground metallic cones were pressed against a polished flat ceramic counterface, using the equipment shown schematically in Fig. 1. The softer cone is flattened to a conforming surface on first application of the maximum load, followed by essentially sinusoidal compressive loading. The reasons for using a softer conical material are:

(a) it is relevant to operational situations where the ceramics are subjected to repeated loading by softer materials, e.g. valve seats in engines;

(b) a harder indentor would produce immediate substantial localized plastic deformation, and possibly concomitant cracking;

(c) the deformation of the softer indentor ensures that there is good conformity and alignment of the two contact surfaces, which results in a uniform pressure distribution, and

(d) the contact area does not vary significantly as the load is cycled in a test, as it would with purely elastic, e.g. Hertzian type, contact.

The test temperatures, 293–1073 K, were chosen to span the likely operational regime for this material and also the transition between stable and metastable tetragonal phases [14, 15].

2. Experimental procedure

2.1. Materials

Compacts of ceria-stabilized polycrystalline zirconia, cold isostatically pressed before being fired at 1723 K,

0022–2461

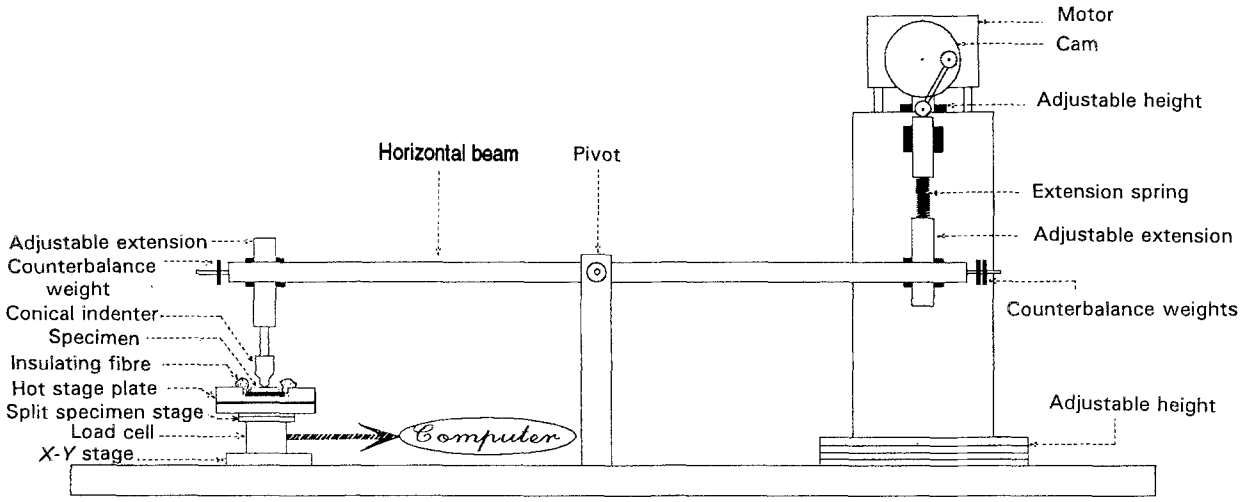

Figure 1 A schematic illustration of the apparatus used for cyclic load fatigue at high temperatures.

were supplied in the form of 60 mm × 60 mm × 5 mm tiles with batch reference UC11. X-ray diffraction studies were performed and the crystal structure was found to be fully tetragonal. A scanning electron microscope (SEM), operating at 30 kV, with associated energy dispersive X-ray analyser (EDX) and ZAF4 software system, was used to determine the grain size and the amount of stabilizing agent. Molten KOH at 400 °C was found to be a suitable etchant for CeTZP. Grains ranging between 1 and 2 μm in size with occasional larger grains (up to 5 μm) were observed. The ceria-stabilized polycrystalline zirconia used in the tests contained 10.45 mol % CeO_2, with a small amount, ~ 1%, of hafnium. The hafnium and cerium ions are both tetravalent like the zirconium, and will replace it substitutionally with no compensating oxygen ion vacancies being required. This composition is consistent with the material being face centred tetragonal [14, 15].

Room-temperature Knoop hardness (19.6 N applied load) and indentation fracture toughness tests, using the Anstis *et al.* analysis [16], were performed on a ground and polished (1/4 μm diamond finish) surface of CeTZP and measured as 8.1 GPa and 15.8 MPa $m^{0.5}$, respectively [17].

The metallic indentors used for repeated point contact loading tests were machined from 12 mm silver steel (BS1407:1970) bars into cones having an apex angle of 120°. The tips were hardened by heating for 1 h at 850 °C, and subsequently quenched in oil. The tips were thereafter carefully ground to a sharp apical angle of 120° and thoroughly cleaned ultrasonically in acetone prior to the cyclic fatigue tests. The sharpness and integrity of the ground tips were ensured by examining their profile under an optical microscope. A longitudinal cross-section of a hardened silver steel tip was prepared for Knoop hardness measurements. Values of 7.6 GPa (applied load 19.6 N) were found around the apex of the tip. The etched microstructure was observed to be lower bainite.

2.2. Test procedure

The repeated point contact loading method has been described previously [13, 18]. In order to conduct tests at elevated temperatures, a Linkam heating stage was inserted into the purpose-designed and built computer-controlled apparatus shown schematically in Fig. 1. The toughened zirconia specimen was firmly glued on to the heating element of the hot-stage plate using fire cement. Both test surfaces were thoroughly cleaned and degreased in acetone. The polished CeTZP surface was not loaded during heat-up or cool-down. It was allowed to equilibrate at the test temperature for at least 1 h before the metallic tips were pressed on to the surface at the mean compressive load (i.e. 19.6 N). The tips were, in turn, allowed to equilibrate at the test temperature for approximately 20 min before the load cycling commenced. A new cone was used for each test.

Compressive cyclic loads of a sinusoidal waveform (2 Hz frequency) were applied to the ceramic substrate by the flattened cone. The compression axis was perpendicular to the polished plane of the CeTZP. The same maximum and minimum loads of 29.4 and 9.8 N, respectively, were used at all temperatures. The load was continuously displayed and recorded using a load cell with a precision of 0.01 N and a 12 bit analogue to digital convertor operating at 100 kHz. The number of cycles varied between 10 and 475 000, depending on the observed damage in the vicinity of the impression. The cone and substrate remained in contact for the entire duration of each test.

Tests were initially conducted at 293 K, followed by 473–1073 K in 200 K increments. The temperature of the ceramic was continuously monitored by a type K thermocouple on the polished substrate close to the point contact loading position.

The same polished CeTZP surface was used throughout the whole temperature range. Accumulated damage and crack morphologies were monitored immediately after each test on the indented surface of the specimen with the aid of an optical microscope for temperatures of 293–673 K. Direct examination for tests performed at 873 and 1073 K was not possible owing to the substantial heat generation from the surface of the ceramic substrate. The CeTZP specimen was slowly cooled down to room temperature after the set of repeated point contact

loadings at a given temperature for SEM observation and EDX analysis. The tested region only of the surface was gold coated prior to this examination.

3. Results and observations

At the commencement of a test the silver steel cone is compressed against the surface of the polished CeTZP substrate, whence the tip of this cone, which has a radius $\leqslant 1$ μm, is flattened to produce a circular conforming planar surface of at least 40 μm diameter. The metal and ceramic then remain in contact for all the load cycles for a particular test. The features observed as a result of this test procedure will be described and thence the relevant measurements pertaining to the observations.

3.1. Observations of deformation and fracture

3.1.1. 293 K

The scanning electron micrographs showing the relevant aspects of the deformation and fracture of the

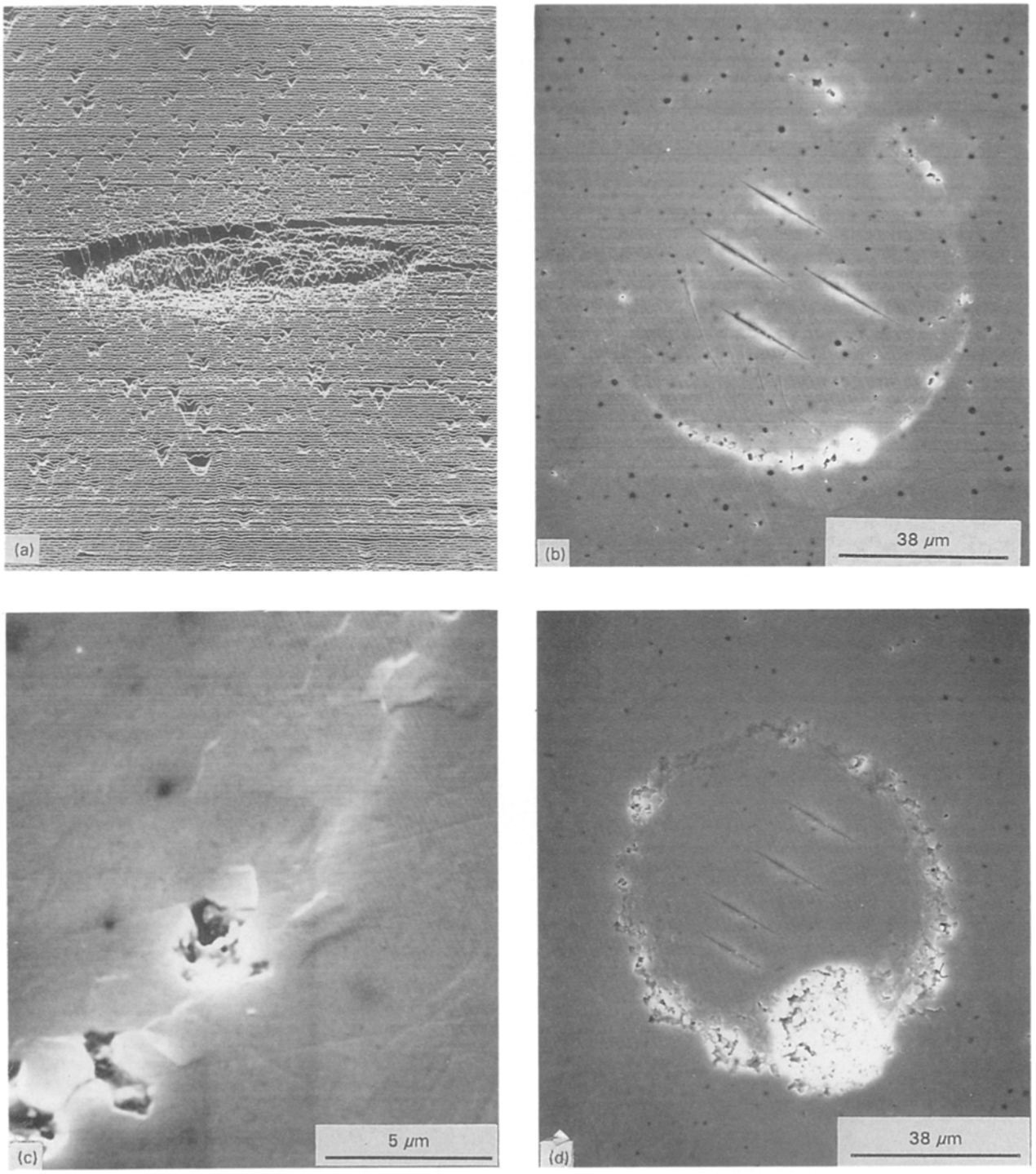

Figure 2 (a–d) Aspects of deformation and fracture caused by 120° hardened silver steel tips on Ce-TZP; frequency, 2 Hz; applied cyclic load 19.6 ± 9.8 N. (a) 12.75×10^4 cycles, SEM line-scan micrograph showing a raised area surrounding the contact zone (note the presence of a Vickers indentation in the centre of the deformed impression). Magn × 800, sample tilt $\approx 90°$. (b) 1×10^4 cycles, microcracking and pitting occur at the edge of the contact zone. (c) 5.70×10^4 cycles, details of the edge of the contact zone showing "uplifting" of some of the grains. (d) 1.50×10^5 cycles, microfracture surrounds the contact zone perimeter and leads to grain chipping.

CeTZP substrate for tests at ambient temperature are presented in Fig. 2. Note that in some cases these figures also show Knoop or Vickers indentations within the contact zone which were performed subsequent to the fatigue testing as discussed below. As can be seen from Fig. 2a, there is a raised area surrounding the contact zone. This region results from the plastic deformation associated with the tetragonal to monoclinic phase transformation [14, 15]. After further cycling, microcracking and pitting are seen to occur, initially at the edge of the contact zone, Fig. 2b. This fragmentation arises from the displacement incompatibilities resulting from this martensitic phase transformation, which cause separation of the grain boundaries close to the surface, with the associated "uplifting" of some of the grains, Fig. 2c. This microfracture initially starts at a small number of sites which then propagates to surround entirely the contact zone perimeter, followed by radial progression both into and away from the contact area, Fig. 2d. EDS analysis of the contact zone on the substrate and the flattened metallic cone tip showed no transfer of material, except for test above 10^5 cycles, where metal adhesion was detected at the edges of the contact zones.

3.1.2. 473 K

The nature of the deformation and fragmentation at this temperature is qualitatively similar to that at 293 K, except that the number of cycles to induce a given degree of deformation or fracture is reduced approximately two- to five-fold. Fig. 3a shows that plastic deformation has occurred after only 10 cycles. There are also some "step-like" features apparent within the contact zone. Microcracking has commenced after 100 cycles at several points on the periphery of the contact zone, Fig. 3b. After 10 000 cycles, the microcracking has linked together somewhat, Fig. 3c, and the raised deformed transformation region around the contact area can be readily discerned, Fig. 3d. This process continues until there is again a substantial intergranular fracture region growing into and away from the contact zone periphery, Fig. 3e and f. A trace amount of iron was again detected around the edges of the contact zone on the CeTZP for the tests above 80 000 cycles.

3.1.3. 673 K

Although similar features to those observed at the lower temperatures are also present at 673 K, there are some differences. The "steps" within the contact zone, noted in Fig. 3a, now appear considerably more pronounced as a "terracing" effect after 1000 cycles, Fig. 4a. Also, in addition to the microcracking observed at the periphery of the contact zone, there are much longer intergranular cracks propagating radially outwards, Fig. 4b. Fragmentation has occurred almost completely around the edge of the contact zone after 10^4 cycles, Fig. 4c. The typical raised transformed areas which are present at the lower temperatures, as shown for example in Fig. 3d, were much less pronounced and difficult to measure at this temperature. Similar to 293 and 473 K, a small amount of iron was detected within the pitted areas subsequent to their formation.

3.1.4. 873 and 1073 K

The form of the deformation and cracking was quite different at these temperatures, and also occurred after

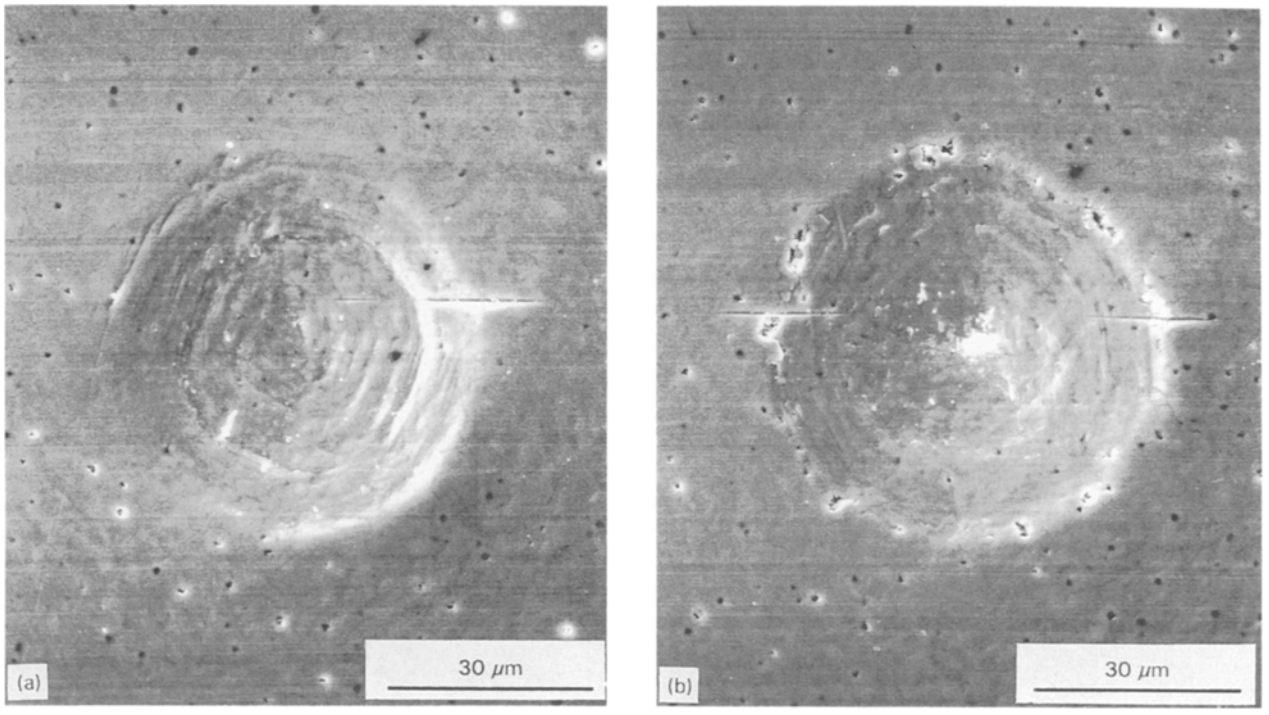

Figure 3 (a–f) The effect of number of cycles on the damage caused on Ce-TZP by 120° hardened silver steel indentors at 473 K; frequency 2 Hz; applied cyclic load 19.6 ± 9.8 N. (a) 10 cycles, (b) 100 cycles, (c) 10^4 cycles. (d) Raised deformed transformation region appears clearly after 10^4 cycles (sample tilt: ≈ 90°). (e) 1.50×10^5 cycles: substantial intergranular fracture propagates into and away from the contact zone periphery. (f) 1.50×10^5 cycles, sample tilt ≈ 90°, micrograph showing raised plastic deformation zone surrounding the impression.

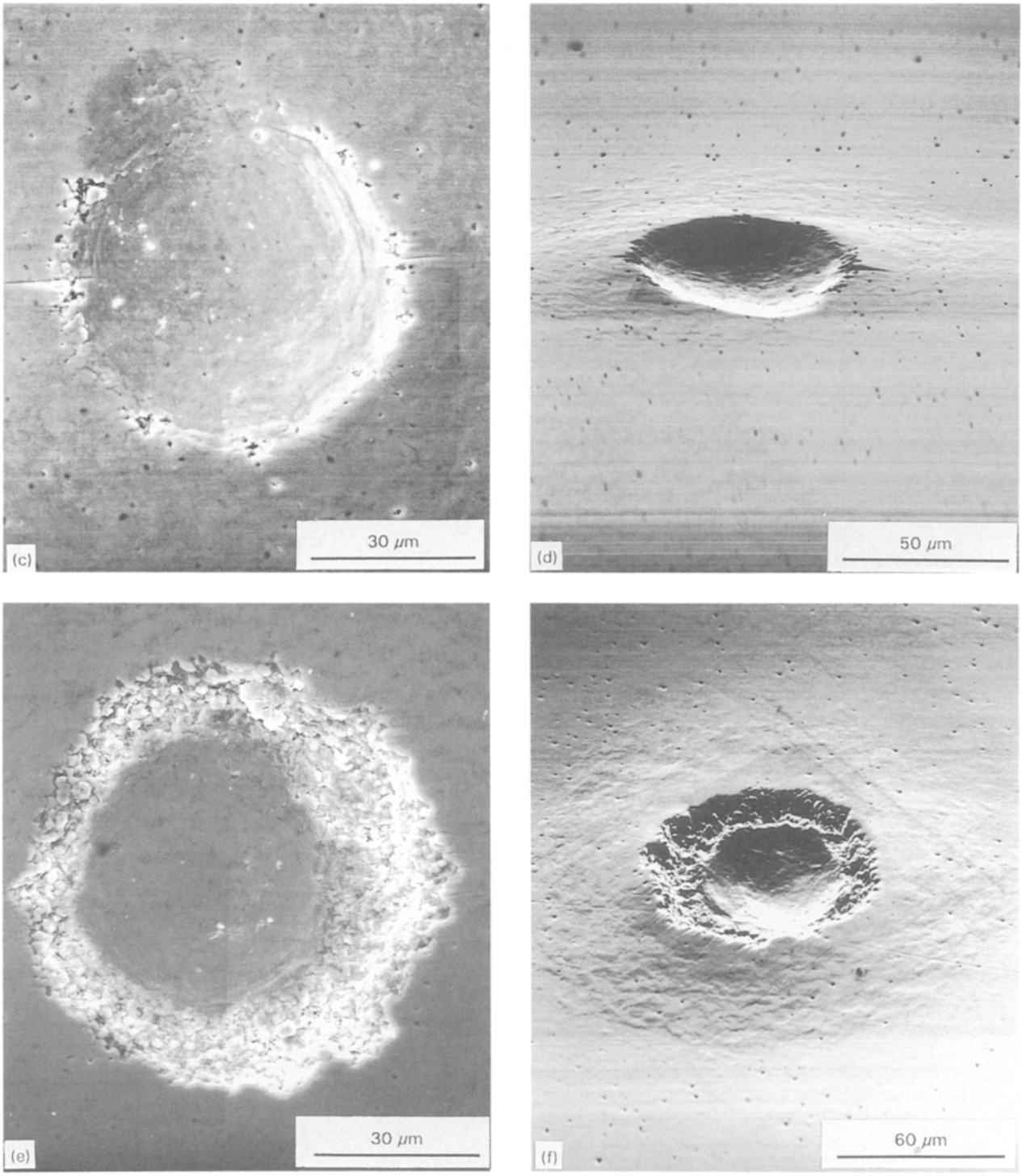

Figure 3 (continued).

relatively few load cycles, Fig. 5. There was no discernible raised transformation zone and the pitting-type microcracking did not occur. Instead, the metallic cone now produced a definite impression in the CeTZP, Fig. 5a, and between three and five radial intergranular cracks were formed, Fig. 5b, which propagated up to $\sim 100\,\mu m$ from the edge of the contact zone, accompanied by tangential cracking within the edges of the contact zone, Fig. 5c. Transfer of iron to the ceramic substrate occurred for all tests and was more noticeable at these temperatures, although the amounts involved were still relatively small.

3.2. Results

The temperature dependence of the Vickers diamond pyramid indentation hardness and toughness of the CeTZP, with a 10 N load, are shown in Fig. 6. It was not possible to initiate cracking at temperatures below 573 K with such a low load. These results are comparable with those of other workers on toughened zirconias [19, 20].

The diameters of the contact zones as measured on the ceramic substrate are shown in Fig. 7. The values for the higher number of cycles at low temperatures are difficult to define owing to the extensive fracture which occurs around the edges of the contact zones.

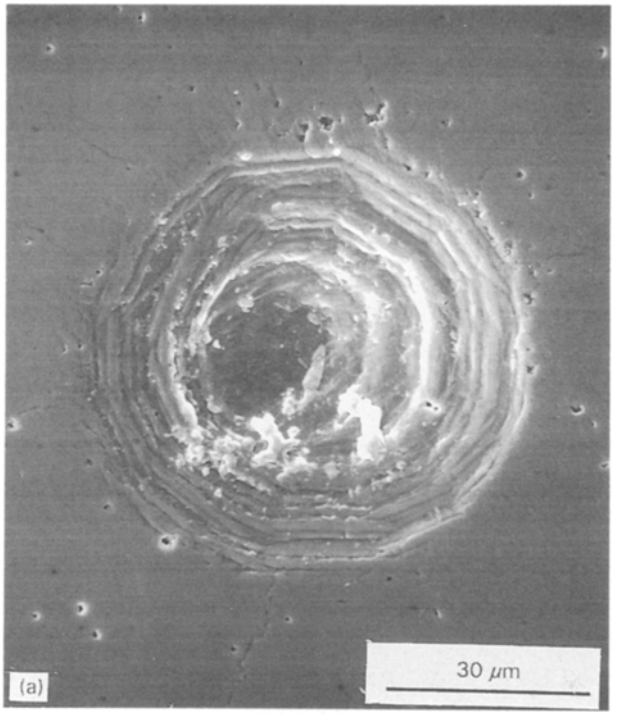

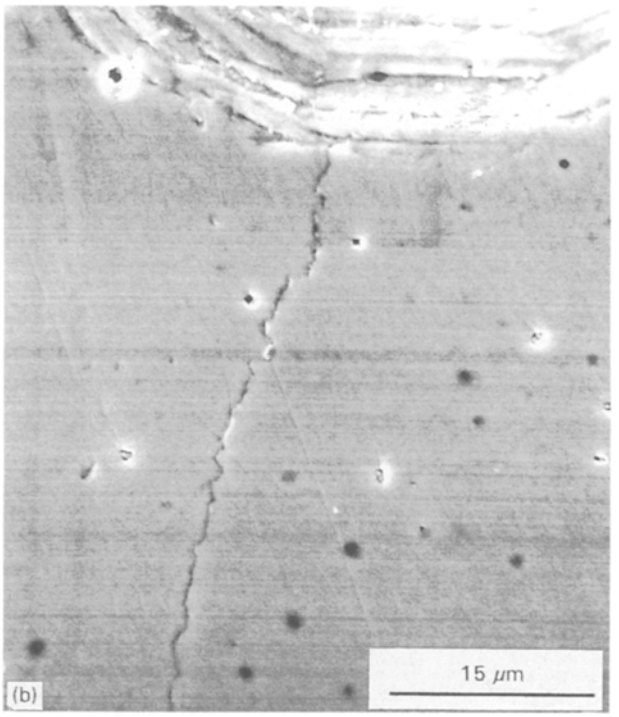

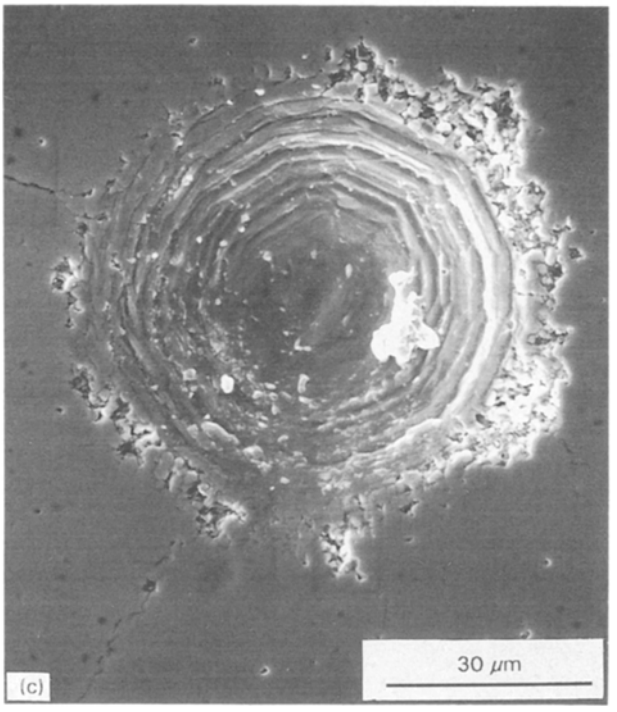

Figure 4 (a–c) The effect of number of cycles on the damage caused on Ce-TZP by 120° hardened silver steel indentors at 673 K; frequency 2 Hz; applied cyclic load 19.6 ± 9.8 N. (a, b) 10^3 cycles; "terracing" features occur within the contact zone (a) and long intergranular cracks are propagating radially outwards (b). (c) 10^4 cycles: fragmentation has occurred almost completely around the edge of the contact zone.

These diameters increase with increasing test temperature and number of cycles. This probably indicates that further spreading of the plastically deformed tip occurs as a result of fatigue in the metallic cone. The corresponding values for the maximum contact pressure at the end of a test, calculated from the maximum load, 29.43 N, divided by the estimated area of the contact zone, are shown in Fig. 8. The minimum and mean contact pressures at the end of each test are one-third and two-thirds, respectively, of the maximum values. The room-temperature values increase with increasing number of cycles. At 473 K this trend is reversed and there is a substantial decrease in the maximum contact pressure with increasing number of cycles. As the test temperature is raised the absolute values of contact pressure decrease and they remain approximately constant at a given temperature, irrespective of the number of cycles. The average values at 673, 873 and 1073 K are 6.4, 4.1 and 2.7 GPa, respectively. These variations arise from the effects of time, temperature and mechanical cycling on the microstructure and plastic deformation of the steel.

The variations of deformed zone sizes with increasing number of cycles for temperatures of 293–673 K are shown in Fig. 9. As mentioned above, precise measurement of these zones is difficult because the transition from raised to level is not well defined, particularly at 673 K. Nevertheless, it would appear that there is an increase in the size of the transformed zone with increasing number of cycles. Also, the diameter of the plastic zone for a given number of cycles increases as the test temperature is raised. Fig. 10 shows the values of Knoop indentation hardness, 0.50 N load, measured within the contact zone for tests performed at room temperature. There is an approximate increase in hardness of 20% as a result of the localized plastic deformation. The change in surface topography after testing at the higher temperatures meant that indentations could not subsequently be made within the contact zone at room temperature. Also, Vickers indentations performed at a sufficiently high load to induce cracking at room temperature were much larger than the contact zone dimensions. Fig. 11 presents the results of the measurements of the

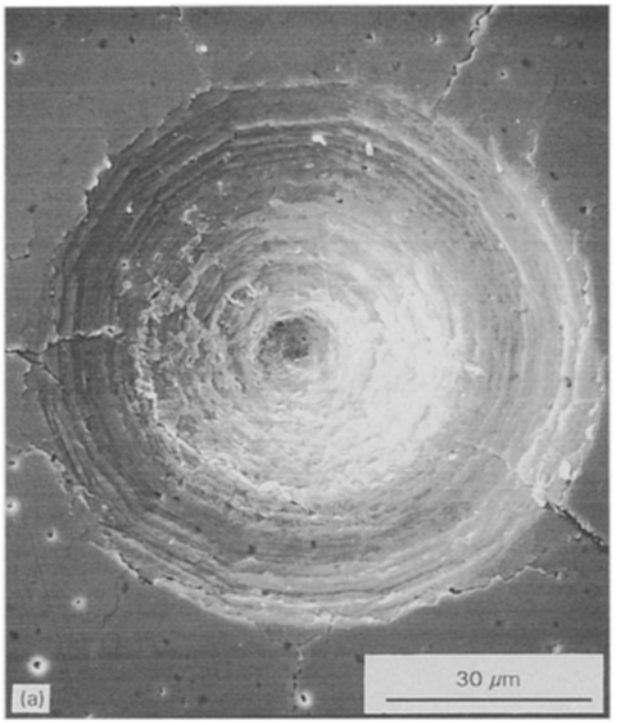

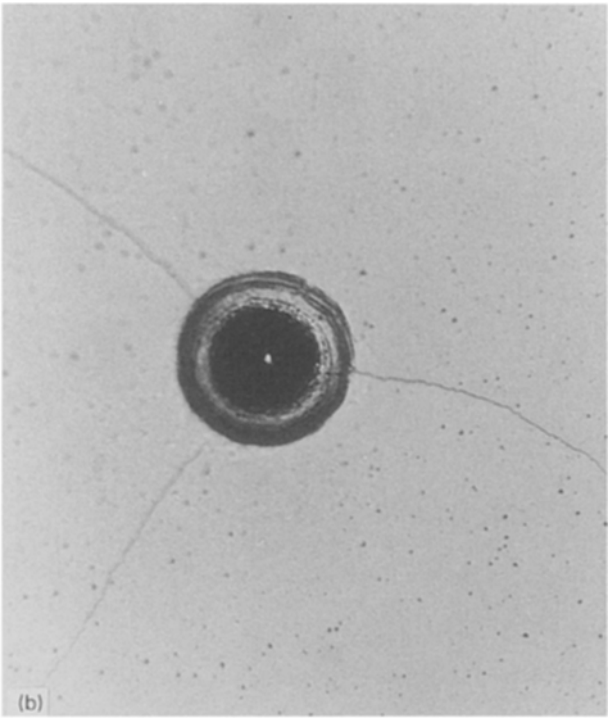

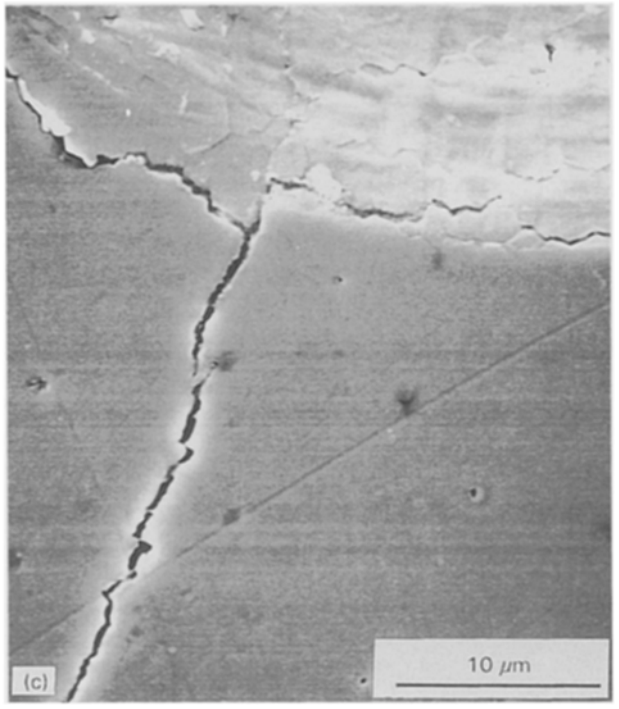

Figure 5 (a–c) The effect of number of cycles on the damage caused on Ce-TZP by 120° hardened silver steel indentors at 873 K; frequency 2 Hz; applied cyclic load 19.6 ± 9.8 N. (a) Deep terraced impression produced after 10 cycles. (b) Optical photograph showing a typical impression and radial cracks produced on CeTZP after 100 cycles at 873 K, Magn × 20. (c) Close-up of both radial and tangential cracking within the edge of the contact zone produced after 100 cycles.

radial cracks observed at 673 K and above. The lengths of the cracks tend to increase with increasing number of cycles, and for a given number of cycles, with increasing test temperature.

4. Discussion

It is apparent in this work that fatigue processes are occurring in this material within the temperature range 293–1073 K. Previous work has shown that the microstructure and room-temperature hardness and toughness are not affected by heating the CeTZP to these temperatures [21]. With this particular sample, a 10^4 cycle fatigue test was performed on the specimen at room temperature after the completion of all the other tests. The deformation and microcracking induced were closely similar to those observed prior to the commencement of the elevated temperature tests.

In the present investigation, the width and depth of the deformed impressions were observed to increase progressively throughout the tests, i.e. the greater the number of compression cycles and/or the higher the temperature, the larger the volumetric displacement of CeTZP material. Fig. 7 shows the effect of the number of cycles on the surface dimension of the impressions performed at different temperatures. In this figure, only the diameter of the indentations was considered, but it is important to point out that the depth of these indentations also increased as both the number of compression cycles and the temperature were raised (see the series of micrographs in Figs 2–5). This has obvious parallels with the observations of Brookes *et al.* [22] for the time-dependent deformation of a hard substrate by a softer deformed cone. Henshall *et al.* [23] have recently demonstrated that the concept of "intrinsic" hardness under these conditions clearly requires redefinition, and the interpretation currently being developed for the static load situation may well be applicable also to the present fatigue test procedure.

From the micrographs described above (Figs 2–5), it is apparent that at temperatures between 293 and 673 K the CeTZP is toughened as a result of the

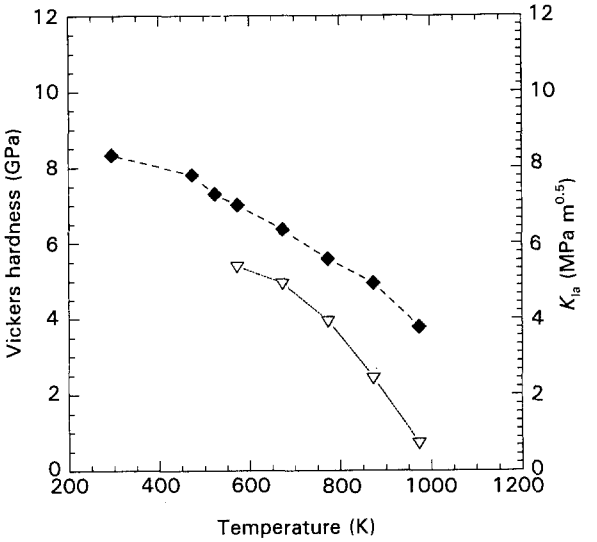

Figure 6 (◆) Vickers hardness and (▽) indentation fracture toughness values [16] versus temperature for a 11.25 mol % CeTZP material. Applied load 10 N; dwell time 12 s.

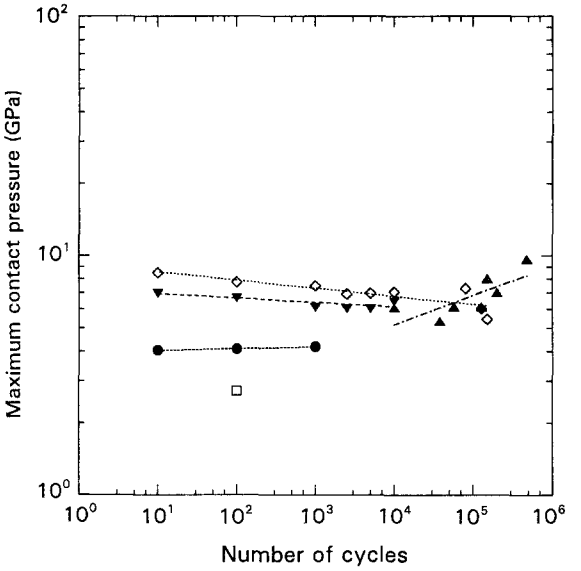

Figure 8 Maximum contact pressure versus number of cycles at (▲) $T = 293$ K, (◇) $T = 473$ K, (▼) $T = 673$ K, (●) $T = 873$ K and (□) $T = 1073$ K; applied cyclic loading 19.6 ± 9.8 N; frequency 2 Hz; substrate CeTZP; 120° hardened silver steel cones; $P_{max} = 29.4$ N.

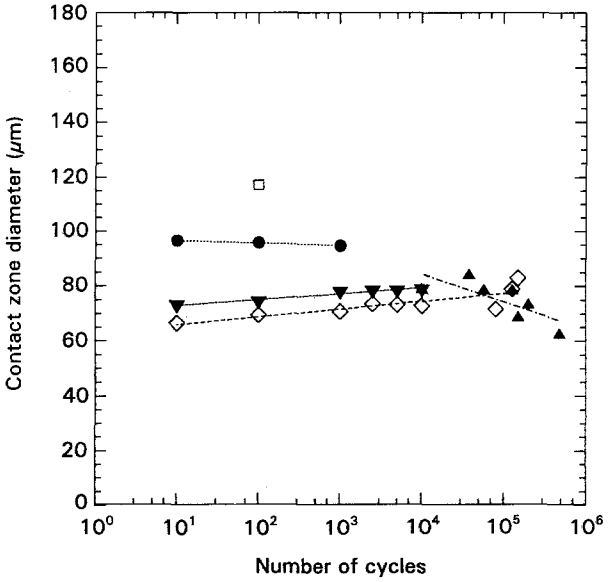

Figure 7 Effect of number of cycles on the diameter of the impressions produced on CeTZP (UC11) using 120° hardened silver steel cones at (▲) $T = 293$ K, (◇) $T = 473$ K, (▼) $T = 673$ K, (●) $T = 873$ K and (□) $T = 1073$ K; cyclic loading 19.6 ± 9.8 N; frequency 2 Hz.

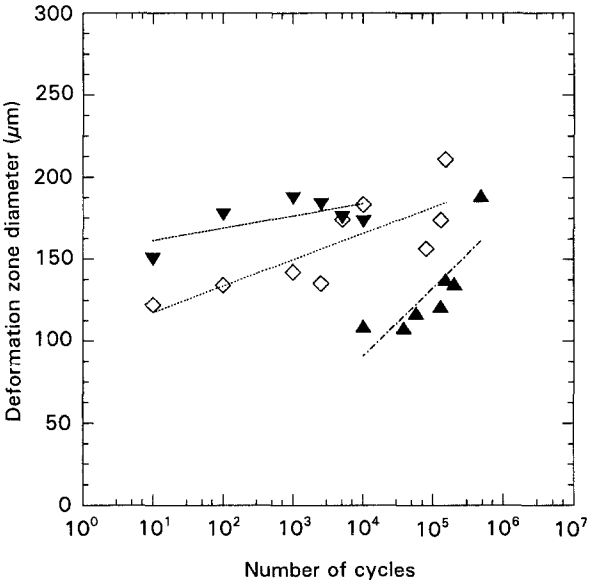

Figure 9 Effect of number of cycles on the diameter of the plastic deformation zones produced on CeTZP (UC11) using 120° hardened silver steel cones at (▲) $T = 293$ K, (◇) $T = 473$ K and (▼) $T = 673$ K; frequency 2 Hz; applied cyclic loading 19.6 ± 9.8 N.

martensitic tetragonal to monoclinic phase transformation. Whether this toughening is entirely due to the energy absorbed by the phase transformation, or is, in part, due to much enhanced local crack roughness, is still not resolved [24]. However, as the test temperature is increased the degree of enhancement of toughness is reduced. It is also quite apparent that the phase transformation occurs before the main crack initiation and propagation stages. Therefore, it is not clear to what extent, if any, the energy absorption involved in the phase transformation can be ascribed to the cracking process as opposed to irreversible (plastic) energy absorption during fatigue. Above 673 K, the tetragonal phase is stable [14, 15] and hence this toughening effect no longer occurs.

673 K lies in the critical regime where, although some transformation, and therefore toughening, was still observed, the cracks that formed propagated well beyond the transformation region. In all cases the cracks/pits that form are intergranular. Initiation occurs at the lower temperatures due to the local strain incompatibilities arising from the stress-induced phase transformation. At the higher temperatures the plastic deformation is most probably controlled by more conventional dislocation processes [25]. Hence crack initiation is most probably related to stress concentrations as a result of dislocation pile-ups, as in MgO [13], which would be expected to predominate at grain interfaces. In both cases the determining factor

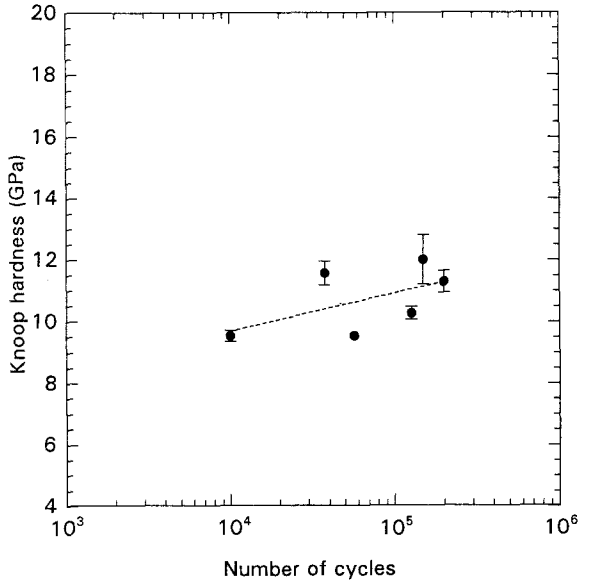

Figure 10 Knoop indentation hardness values measured within the deformed contact zones in CeTZP for tests performed at room temperature versus number of cycles. Applied load 0.50 N; dwell time 12 s.

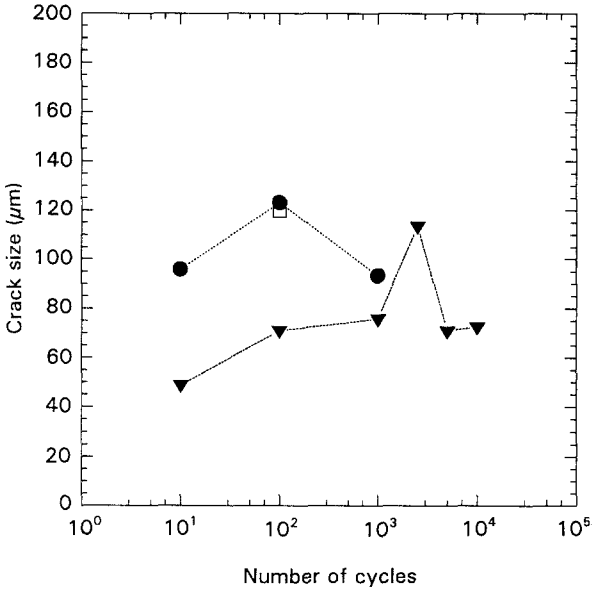

Figure 11 Radial crack size in CeTZP versus number of cycles at (▼) $T = 673$ K, (●) $T = 873$ K and (□) $T = 1073$ K; applied cyclic loading 19.6 ± 9.8 N; frequency 2 Hz.

in the initiation of the first microcracks is the strength/toughness of the grain-boundary regions. As with most ceramics, it has been shown that impurity elements segregate to the grain-boundary regions during sintering [26], and hence relatively small changes in composition may have a strong influence on intergrain bonding, and hence the number of cycles required to induce cracking in these materials in this type of test. At the lower test temperatures, $\leqslant 673$ K, there is no adhesion between the steel and CeTZP until significant surface pitting has occurred, whence metal transfer will happen as a result of deformation and mechanical interlocking of the steel with the roughened ceramic surface. Above 673 K, limited adhesion and metal transfer occurred, but this was clearly an adjunct of the changes in deformation and fracture patterns observed, rather than a determining factor.

The general observations in this work are similar to those of other workers who have studied fatigue in toughened zirconia ceramics in tension or notched/unnotched beams subjected to cyclic bending loads [2–8], where it has been noted that the phase transformation is initiated by either tensile or compressive stresses before cracking occurs, and that at temperatures above ~ 600 K no transformation is observed [8]. The fracture morphology is very similar to that alluded to briefly by Stevens [1] for a TZP cam follower that had been engine tested. This would confirm that the present test method is relevant to in-service performance, but that the test conditions are obviously more controllable and reproducible.

The stress distributions arising from various forms of loaded surface contacts have been summarized by Johnson [27]. It can be assumed that the maximum stress immediately beneath the deformed cone will be compressive and uniform, at least at low temperatures, and of magnitude $\sigma_{zz} = P/\pi r_c^2$, where P is the applied load and r_c is the radius of the contact zone. If the effects of plastic deformation outside the contact zone are ignored, then, for any axially symmetrical pressure distribution within the contact zone, the surface stress distributions outside the contact area are given by [27]

$$\sigma_{rr} = -\sigma_{\theta\theta} = (1 - 2\nu)P/2\pi r^2 \qquad (1)$$

where ν is Poisson's ratio (= 0.27), r is the distance from the centre of the contact, and $\sigma_{zz} = 0$.

The values of the maximum tensile stress, σ_{rr}, at the microcracking/pitting initiation region at 293–1073 K and the ends of the radial cracks at 673 K and above, are shown in Fig. 12. The average stress, minimum

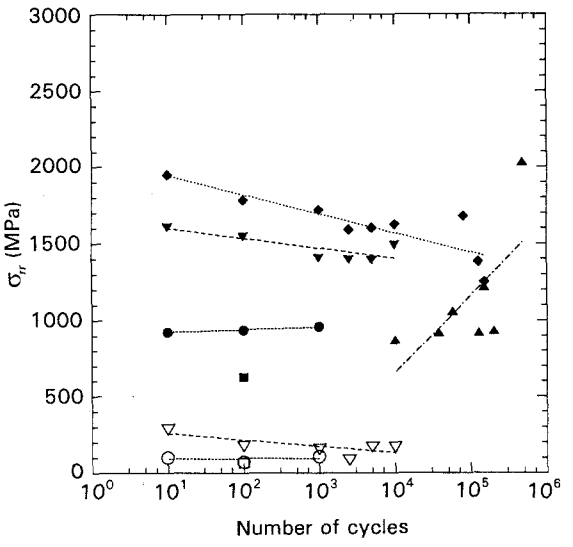

Figure 12 Maximum tensile stresses versus number of cycles at (▲) $T = 293$ K, (◆) $T = 473$ K, (▼) $T = 673$ K, (●) $T = 873$ K and (■) $T = 1073$ K. The open symbols represent values of σ_{rr} at the ends of the radial cracks at (▽) $T = 673$ K, (○) $T = 873$ K and (□) $T = 1073$ K; applied cyclic loading 19.6 ± 9.8 N; frequency 2 Hz; substrate CeTZP; 120° hardened silver steel cones; $P_{max} = 29.4$ N.

stress, and cyclic stress amplitude are two-thirds, one-third and one-third, respectively, of these maximum values. At room temperature there is a substantial scatter in the data, with the average stress at the crack initiation radius being 980 MPa (excluding the value at 475 000 cycles where there is too much fragmentation to be able to define the initiation point with sufficient accuracy). At 473 and 673 K, there would appear to be reasonably uniform decreases in the crack initiation stresses from 1950 MPa to 1250 MPa and 1620 MPa to 1400 MPa, respectively, with increasing number of cycles. At 873 and 1073 K, the stresses are approximately constant at 941 and 630 MPa, respectively. This analysis assumes, of course, that the deformation is purely elastic. The effect of the plastic deformation will be to reduce these estimated values. The stresses at the edges of the radial crack tips are much lower, varying from 300 MPa at 673 K to 68 MPa at 1073 K. The grain "uplifting" and pitting-type fracture occur where the tensile stresses are a maximum, the position of which is largely controlled by the plastic deformation of the conical tips. As the temperature is raised, the stresses at the end of the radial crack tips become relatively low. This presumably reflects a further decrease in the critical stress intensity factor with increasing temperature.

The stress values shown in Fig. 12 can also be used to provide estimates of the working/design stresses to avoid fatigue damage in components operating under these type of contact conditions for fatigue lifetimes of $\sim 10^5$–10^6 cycles.

5. Conclusions

The results presented here have demonstrated the existence of mechanical fatigue effects in a ceria-stabilized tetragonal polycrystalline zirconia for temperatures ranging between 293 and 1073 K. The method of repeated "soft" point contact loading has been demonstrated to be eminently suited to the investigation of the damage accumulated around the contact zones and the propagation of cracks as a function of temperature.

The application of fluctuating compressive loads to CeTZP involved a volumetric displacement of both the deformed impressions and also the plastic deformation zone. The width and depth of the impressions increased as the number of compression cycles and the temperature increased. At 293–673 K, a stress-induced tetragonal to monoclinic martensitic transformation zone was produced around the deformed and growing impressions and expanded both sideways and upwards as the number of cycles was increased. In addition, significant spalling of the grains occurred at the edge of the contact zones beyond $\sim 10^5$ cycles at room temperature. The tetragonal to monoclinic phase transformation toughening did not occur for tests performed above 673 K. Subsequent erratic fragmentation ensued readily.

The mode of fracture was observed to be intergranular in CeTZP. It was noted that a continuation of cyclic compression (beyond the first ten cycles) led to further crack advance at a progressively decreasing rate before arresting completely and the crack length/indentation size ratio was approximately constant with increasing temperature.

The raised plastic deformation zone expanded as the number of compressive cycles increased. This zone became less well-defined as the temperature increased and disappeared completely above 673 K. The fall in the fracture resistance of the CeTZP specimen subjected to repeated compressive point contact loading as the temperature was increased, was most marked. This is attributed to the absence of the transformation toughening above 673 K. The presence or absence of plastic deformation by martensitic phase transformation plays an important role in the fracture processes observed. When a plastic deformation zone exists around the impressions, a significant amount of spalling of the CeTZP grains occurred followed by surface chipping. In the absence of a transformed zone around the impressions, long narrow cracks emanate from the edge of the contact zones, even after only 10 cycles. This behaviour reflects the effectiveness of the tetragonal to monoclinic martensitic phase transformation in restraining catastrophic fatigue crack growth below 673 K and substituting it by grain spalling and chipping at a relatively high number of cycles.

References

1. R. STEVENS, "Zirconia and Zirconia Ceramics", 2nd Edn (Magnesium Elektron, Twickenham, 1986).
2. L. A. SYLVA and S. SURESH, *J. Mater. Sci.* **24** (1989) 1729.
3. K. MAJIMA, K. AMAFUYI, H. NAGAI and K. SHOJI, *J. Mater. Sci. Lett.* **8** (1989) 183.
4. R. H. DAUSKARDT, W. YU and R. O. RITCHIE, *J. Am. Ceram. Soc.* **70** (1987) C248.
5. T. LIU and G. GRATWOHL, in "Fatigue of Advanced Materials: Proceedings of the Engineering Foundation International Conference", Santa Barbara, California, edited by R. O. Ritchie, R. H. Dauskardt and B. N. Cox (Materials and Component Engineering Publications, Birmingham, 1991) p. 265.
6. S. Y. LIU and I. W. CHEN, *J. Am. Ceram. Soc.* **75** (1992) 1191.
7. G. GRATWOHL and T. LIU, *ibid.* **74** (1991) 3028.
8. D. C. CARDONA, P. BOWEN and C. J. BEEVERS, in "Fatigue of Advanced Materials: Proceedings of the Engineering Foundation International Conference", Santa Barbara, California, edited by R. O. Ritchie, R. H. Dauskardt and B. N. Cox (Materials and Component Engineering Publications, Birmingham, 1991) p. 287.
9. G. M. CARTER, R. M. HOOPER, J. L. HENSHALL and M.-O. GUILLOU, *Wear* **148** (1991) 147.
10. C. A. BROOKES, M. P. SHAW and P. E. TANNER, *Proc. R. Soc. Lond.* **A409** (1987) 141.
11. M. REECE and F. GUIU, *J. Am. Ceram. Soc.* **73** (1990) 1004.
12. E. TAKAKURA and S. HORIBE, *J. Mater. Sci.* **27** (1992) 6151.
13. M.-O. GUILLOU, J. L. HENSHALL and R. M. HOOPER, *J. Am. Ceram. Soc.* **76** (1993) 1832.
14. T. K. GUPTA and C. A. ANDERSON, in "Advances in Cryogenic Engineering: Proceedings of the Fifth International Cryogenic Materials Conference", Vol. 30, edited by A. F. Clark and R. P. Reed (Plenum, New York, 1984) p. 367.
15. P. DURAN, M. GONZALEZ, C. MOURE, J. R. JURADO and C. PASCUAL, *J. Mater. Sci.* **25** (1990) 5001.
16. G. R. ANSTIS, P. CHANTIKUL, B. R. LAWN and D. B. MARSHALL, *J. Am. Ceram. Soc.* **64** (1981) 533.
17. M.-O. GUILLOU, J. L. HENSHALL, R. M. HOOPER and G. M. CARTER, *J. Hard Mater.* **3** (1992) 421.

18. M.-O. GUILLOU, J. L. HENSHALL and R. M. HOOPER, *Wear*, **170** (1993) 247.
19. F. F. LANGE, *J. Mater. Sci.* **17** (1982) 255.
20. V. TIKARE and A. H. HEUER, *J. Am. Ceram. Soc.* **74** (1991) 593.
21. M.-O. GUILLOU, PhD thesis, University of Exeter (1992).
22. C. A. BROOKES, E. J. BROOKES, V. R. HOWES, S. G. ROBERTS and C. P. WADDINGTON, *J. Hard Mater.* **1** (1990) 3.
23. J. L. HENSHALL, R. M. HOOPER, K. E. EASTERLING and W. B. LI, *ibid.* **4** (1993) 1.
24. F. GUIU and R. N. STEVENS, *J. Mater. Sci.* **26** (1991) 4375.
25. A. H. HEUER, M. RUHLE and D. B. MARSHALL, *J. Am. Ceram. Soc.* **73** (1990) 1084.
26. J. WANG, H. P. LI, R. STEVENS, C. B. PONTON and P. M. MARQUIS, in "Engineering Ceramics: Fabrication, Science and Technology", edited by D. P. Thompson (Institute of Materials, London, 1993), *Brit. Ceram. Proc.* **50**, p. 161.
27. K. L. JOHNSON, "Contact Mechanics" (Cambridge University Press, Cambridge, 1987).

Recieved 13 October 1993
and accepted 16 June 1994